

# Study of Material Property of Concrete Filled Steel Tubular Columns

Lemya Musthafa<sup>1</sup>, Sunitha Rani C.M<sup>2</sup>, Smitha.K.K<sup>3</sup>

<sup>1</sup>M.Tech Scholar, Dept. of Civil Engineering, KMEA Engineering College, Kerala, India

<sup>2</sup>Assoc. Professor, Dept. of Civil Engineering, KMEA Engineering College, Kerala, India

<sup>3</sup>Assoc. Professor, Dept. of Naval Architecture & Ship Building Engineering, SNGC Engineering College, Kerala, India

\*\*\*

**Abstract** - In recent years, a type of hybrid system, the concrete-filled steel tubular (CFST) columns are increasingly used in buildings and bridges. In CFST columns, the steel tube provides formwork for the concrete, the concrete prolongs local buckling of the steel tube wall, the tube prohibits excessive concrete spalling, and composite columns add significant stiffness to a frame compared to more traditional steel frame construction. The paper presents a non-linear finite element analysis of circular and square CFST columns using commercial finite element software, ANSYS. The study focuses on the material property of CFST columns.

**Key Words:** CFST, ANSYS, axial load, non-linear analysis, confinement

## 1.INTRODUCTION

Due to rapid advancement of concrete technology, high-performance concrete, which has high strength, has gradually become a central element in structural systems. However, a higher strength concrete is generally more brittle and for this reason, there has been hesitation in the use of high-performance concrete with strength higher than a certain limit. To ensure minimum ductility, transverse reinforcement for confining the concrete has to be provided. But, as the strength of concrete improves, the demand for transverse reinforcement also increases. Moreover, closely spaced transverse reinforcement would lead to steel congestion inside the mould, thus posing difficulties in concrete casting. Therefore, it has been advocated to adopt the concrete-filled steel tube system to provide confinement to concrete columns without causing steel congestion inside the mould.

**Concrete-Filled Steel Tubes (CFST)** are composite members consisting of a steel tube infilled with concrete, possessing the favorable attributes of both concrete and steel. The continuous confinement provided to the concrete core by the steel tube enhances the core strength and ductility. The concrete core restrains inward buckling of the steel tube, while the steel tube serves as tensile reinforcement for the concrete.

The steel lies at the outer perimeter where it performs most effectively in tension and in resisting bending moment. Also, the stiffness of the CFST is greatly enhanced because the steel, which has a much greater modulus of elasticity than

the concrete, is situated farthest from the centroid, where it makes the greatest contribution to the moment of inertia. The concrete forms an ideal core to withstand the compressive loading in typical applications, and it delays and often prevents local buckling of the steel.

It provides not only an increase in the load carrying capacity but also economy and rapid construction, and thus additional cost saving. Their use in multistory buildings has increased in recent years owing to the benefit of increased load carrying capacity for a reduced cross section.

The CFST columns do not require formwork and additional steel reinforcement, and the steel tube protects its surface from impact and abrasion. The local buckling of the steel wall, due to the relatively small wall thickness, is delayed because the inward buckling is resisted by concrete.

The relevance of this topic is due to the enhancement in structural properties of CFST due to the interaction between steel tube & concrete core. They combine the advantages of ductility of steel & stiffness of concrete. There are several advantages which justify the use of CFST. Some of these advantages include:

- Greater energy dissipation and fire resistance
- Drying shrinkage & creep of concrete in CFST is much smaller
- Higher strength-to-weight ratio
- Higher rigidity than conventional reinforced concrete column
- High ductility and toughness for resisting reversal load
- Excellent structural performance, such as high strength, high ductility and large energy absorption capacity
- Higher load carrying capacity due to the composite action between steel and concrete
- Concrete casting is done by tremie tube /pump-up method which result in reduction in manpower & cleaner construction sites
- Saving in material and construction time

## 2. PREVIOUS RESEARCH

The studies on CFST columns had started since 1980s, due to its wide applications many researchers have conducted experiments to study different parameters of CFST columns. Most of the researches were focusing stub columns.

The circular steel tubes offer much more post-yield axial ductility than the square or rectangular tube sections. For small dimensional CFST columns, smaller  $D/t$  ratios provide a significant increase in yield load and more favorable post-yield behavior [8]. The difference between the ultimate strength of circular and rectangular CFST columns, can be estimated as a linear function of the tube yield strength. A stress-strain model for a square steel tube was also formulated based on the experimental results [12]. Axial capacity of CFST columns are significantly affected with the cross-section of the column [22].

The increase in column slenderness decreases the load carrying capacity of composite column [13]. The area of steel should be at least 13% of the total area of composite section with cross section to thickness ratio  $(B/t) \leq 30$  to enhance the load carrying capacity and ductility of CFST [24].

Concrete compressive strength is the important factor affecting the descending region of the stress-strain curves for CFST. The lateral displacement in the rectangular CFST's is more susceptible to the steel tube thickness than the longitudinal displacement. The Failure of CFST's is initiated by local buckling in the middle third of height, in which the stresses are concentrated [19]. The deformation decreases by increase in the grade of concrete [14, 17, 21, 25]. But for higher grades of concrete deformation almost reads constant [26].

The effect of yield stress of steel tube in CFST columns on improving the concrete ductility is more significant than its effect on increasing the axial load carrying capacity of the column. The results indicated that the most reasonable steel grade for the purpose of ductility seems to be Grade 52, and use of steel tube with high yield stress is not necessary [18].

Ying Wang (2010) added the bonding element to simulate the bond-slip behavior between steel and concrete, such as the COMBIN39 element, TARGE170 element and CONTA173 element [16], in the non-linear analysis of CFST.

The design method given in ACI-318 codes [1] is highly conservative for estimating the ultimate axial strengths of circular CFSST short columns because the codes do not account for the concrete confinement effects and significant strain hardening of stainless steels in compression. Eurocode 4 [3] considers the effects of concrete confinement in the calculation of the ultimate axial strength of circular concrete-filled steel columns. However, it still provides conservative design strengths since the significant strain hardening of stainless steel has not been taken into account in Eurocode 4 [27].

An accurate formula for predicting the axial capacity of circular CFST stub columns with normal- and high-strength steel and concrete was proposed [15]. The scale effect on the strength of the filled concrete and enhancement of strength of CFST columns due to the composite action between steel tube and concrete core are taken into account in the proposed formula.

Local buckling of steel tubes was effectively delayed by the stiffeners, thus the stiffened columns have higher serviceability benefits compared to those unstiffened ones [10]. The load-carrying capacity of the composite columns was increased when stiffeners were provided, and the ductility can also be increased slightly [14].

U-links modified the flexural behaviour of the composite member, not only because they contribute to the compressive strength of concrete by confining it, but also because they delay, and even prevent, the local buckling of the steel in compression by supporting it laterally along with the concrete core [20].

## 3. NON-LINEAR ANALYSIS OF CFST COLUMNS UNDER AXIAL LOAD

### 3.1 Design considerations:

#### 3.1.1 Steel

The outer profile of the steel tube should not be too small in order to allow proper concrete placement. On the other hand, the wall thickness of the steel tube should exceed a certain value to ensure the stability. According to the DBJ/T 13-51 specification [2], a Chinese local specification for CFST structures, the outer profile of the steel tube should be not less than 100 mm, and the wall thickness of the steel tube for hot-finished and cold-formed sections should not be less than 4 mm and 3 mm, respectively.

In the DBJ/T 13-51 specification [2],

For concrete-filled steel tubular columns:

$$\text{circular sections, } \frac{D}{t} \leq 150 \frac{235}{f_y} \quad (1a)$$

$$\text{square sections, } \frac{B}{t} \leq 60 \frac{235}{f_y} \quad (1b)$$

where,  $D$  is the outer diameter of the circular

$B$  is the depth of rectangular sections

$t$  is the wall thickness of the tube

$f_y$  is the yield strength of steel.

If the  $D/t$  ratio exceeds the limitations, additional longitudinal stiffeners shall be designed and provided.

#### 3.1.2 Concrete

The normal weight concrete and the high-strength concrete can be used as the filled concrete in CFST structures. Since

the excess water cannot be expelled from the sealed tube, the water to cement ratio of the concrete should be strictly controlled. A water to cement ratio exceeding 0.4 is inappropriate for normal weight concrete. It is recommended that the strength of the steel and the concrete should be suitably matched to improve the structural performance. It is appropriate to use the combinations of higher strength steel with higher strength concrete, and lower strength steel with lower strength concrete.

### 3.2 Material Modelling

The contact between steel tube and concrete causes composite action between steel and concrete in a CFST column. The radial lateral confining pressure exerted by the steel tube on the concrete induces confinement in concrete. Thus, to effectively replicate the inherent advantages of CFT, it is necessary that the composite action between steel and concrete be very carefully modelled.

#### 3.2.1 Concrete Modelling

The uniaxial behaviour of the steel box is simulated by an elastic-perfectly plastic model. The equivalent uniaxial stress-strain curves for both unconfined and confined concrete are shown in Fig. 1, where  $f'_c$  is the unconfined concrete cylinder compressive strength. The corresponding unconfined strain ( $\epsilon'_c$ ) is taken as 0.003. The confined concrete compressive strength ( $f'_{cc}$ ) and the corresponding confined strain ( $\epsilon'_{cc}$ ) can be determined from Eqs. (2) and (3) respectively [10],

$$f'_{cc} = f'_c + k_1 f_l \tag{2}$$

$$\epsilon'_{cc} = \epsilon'_c (1 + k_2 \frac{f_l}{f'_c}) \tag{3}$$

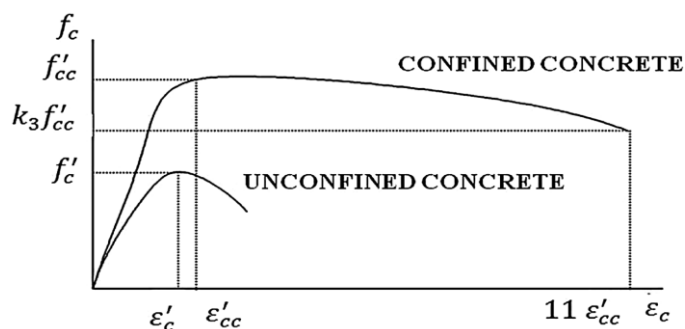


**Fig. 1** Uniaxial stress-strain curves for confined and unconfined concrete[11]

The confinement coefficients,  $k_1$  and  $k_2$  are constants and can be obtained from experimental data. Meanwhile, the constants  $k_1$  and  $k_2$  were set as 4.1 and 20.5 based on the studies of Richart [5], where  $f_l$  represents the lateral confining pressure around the concrete core, calculated from the following empirical Eqs. 4a and 4b for CFST columns with unstiffened square sections [11]:

$$\frac{f_l}{f_y} = [0.055048 - 0.001885(B/t)] \text{ for } 17 \leq B/t \leq 29.2 \tag{4a}$$

$$\frac{f_l}{f_y} = 0 \text{ for } 29.2 \leq B/t \leq 150 \tag{4b}$$

The confining pressure around the concrete core can also be determined from the following empirical Eqs. (5a) and (5b) for CFST columns with unstiffened circular sections:

$$\frac{f_l}{f_y} = [0.043646 - 0.000832(D/t)] \text{ for } 21.7 \leq D/t \leq 47 \tag{5a}$$

$$\frac{f_l}{f_y} = [0.006241 - 0.0000357(D/t)] \text{ for } 47 \leq D/t \leq 150 \tag{5b}$$

To define the full equivalent uniaxial stress-strain curve for confined concrete as shown in Fig. 1, three parts of the curve have to be identified. The first part is the initially assumed elastic range to the proportional limit stress. The proportional limit stress is taken ( $0.5 f'_{cc}$ ) [11]. The initial Young's modulus of confined concrete ( $E_{cc}$ ) is reasonably calculated using the empirical Eq. (6). The Poisson's ratio ( $\mu_{cc}$ ) of confined concrete is taken as 0.2. [11].

$$E_{cc} = 4700 \sqrt{f'_{cc}} \text{ MPa} \tag{6}$$

The second part of the curve is the nonlinear portion starting from the proportional limit stress  $0.5 (f'_{cc})$  to the maximum confined concrete strength ( $f'_{cc}$ ). The compressive strength ( $f$ ) in the nonlinear portion can be determined from Eq. (7), suggested by Saenz [6],

$$f = \frac{(E_{cc} \epsilon)}{\{1 + (R + R_E - 2) \left(\frac{\epsilon'_c}{\epsilon'_{cc}}\right) - (2R - 1) \left(\frac{\epsilon'_c}{\epsilon'_{cc}}\right)^2 + R \left(\frac{\epsilon'_c}{\epsilon'_{cc}}\right)^3\}} \tag{7}$$

$$R = \frac{R_E (R_\sigma - 1)}{R_E} - \frac{1}{R_E} \tag{8}$$

$$R_E = \frac{E_c \epsilon'_{cc}}{f'_{cc}} \tag{9}$$

$R_\sigma$  and  $R_E$  are taken equal to 4, as suggested Elwi and Murray [7]

The last part of the curve, the descending line is assumed to be terminated at the point where

$$f_c = k_3 f_{cc} \tag{10}$$

$$\epsilon_c = 11 \epsilon'_{cc} \tag{11}$$

The values for  $f_l$  and  $k_3$  have to be provided to completely define the uniaxial stress-strain relation. These two parameters are apparently dependent on the confining pressure, which varies during loading and depends on the  $B/t$  or  $D/t$ , cross-sectional shape, and stiffening means.

The material degradation parameter,  $k_3$  can be calculated, from the following empirical equations (12 a) and (12 b) for square, (13 a) and (13 b) for circular [11]:

For square sections,

$$k_3 = 0.000178 (B/t)^2 - 0.02492 (B/t) + 1.2722 \quad (17 \leq B/t \leq 70) \quad (12 \text{ a})$$

$$k_3 = 0 \quad (70 \leq B/t \leq 150) \quad (12 \text{ b})$$

For circular sections,

$$k_3 = 1 \quad (27.7 \leq D/t < 40) \quad (13 \text{ a})$$

$$k_3 = 0.0000339 (D/t)^2 - 0.010085 (D/t) + 1.3491 \quad (40 \leq D/t \leq 150) \quad (13 \text{ b})$$

It can be observed that both the lateral confining pressure  $f_l$  and the material degradation parameter  $k_3$  will be higher for circular section when compared to square section. For columns with circular or square section both  $f_l$  and  $k_3$  decrease with increasing  $D/t$  or  $B/t$  ratio. When the  $D/t$  or  $B/t$  ratio is small,  $f_l$  and  $k_3$  tend to be large due to the lateral confinement from the steel tube. When the  $D/t$  or  $B/t$  ratio is large,  $f_l$  and  $k_3$  tend to be small due to the lack of lateral support from the tube.

Because the concrete in the CFT columns is usually subjected to triaxial compressive stresses, the failure of concrete is dominated by the compressive failure surface expanding with increasing hydrostatic pressure. Hence, a Drucker-Prager (DP) yield criterion is used to model the yield surface of concrete which assumes an elastic perfectly plastic response [9]. The yielding surface of the DP criterion may be considered depending on the internal friction angle of the material and its cohesion. The amount of dilatancy (the increase in material volume due to yielding) can be controlled with the dilatancy angle.

The material parameters cohesion ( $c$ ), angle of internal friction ( $\varphi$ ) [9] and dilatancy angle ( $\psi$ ) [23] for the DP model can be calculated from Eqs. (14) to (16) suggested by the researchers:

$$\varphi = \sin^{-1} \left[ \frac{3}{1 + \frac{2f'_c}{\sqrt{3}}} \right] \quad (14)$$

$$c = (f'_c - 5\sqrt{3}) \frac{3 - \sin \varphi}{6 \cos \varphi} \quad (15)$$

where,  $f'_c$  and  $c$  the cohesion calculated is in MPa and  $\varphi$  is in degrees.

$$\psi = 56.3 (1 - \xi_c) \quad \xi_c \leq 0.5 \quad (16 \text{ a})$$

$$= 6.672 e^{\left( \frac{7.4}{4.64 + \xi_c} \right)} \quad \xi_c > 0.5 \quad (16 \text{ b})$$

where, the confinement factor  $\xi_c$  is expressed as:

$$\xi_c = \frac{A_s f_y}{A_c f'_c} \quad (17)$$

### 3.2.2 Steel Modelling

The bilinear kinematic hardening model as shown in Fig. 2 was used to simulate the stress-strain curve of steel and assumed to be an elastic-perfectly plastic material. The

bilinear model requires the yield stress ( $f_y$ ) and the hardening modulus of the steel ( $E_s$ ), the Constitutive law for steel behaviour is:

$$\sigma_s = E_s \varepsilon'_s \quad \varepsilon_s \leq \varepsilon_y \quad (18)$$

$$\sigma_s = f_y + E'_s \varepsilon'_s \quad \varepsilon_s > \varepsilon_y \quad (19)$$

Where,  $\sigma_s$  is the steel stress,  $\varepsilon_s$  is the steel strain,  $E_s$  is the elastic modulus of steel,  $E'_s$  is the tangent modulus of steel after yielding,  $E'_s = 0.01E_s$ ,  $f_y$  and  $\varepsilon_y$  are the yielding stress and strain of steel, respectively.

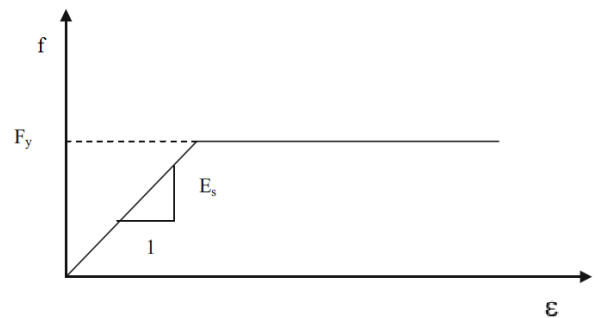


Fig.2. Elastic perfectly plastic model for steel tube

## 4. FINITE ELEMENT ANALYSIS

The Concrete filled Steel Tube (CFST) was modelled using the finite element software ANSYS 14. ANSYS is a commercial FEM package having the capabilities ranging from a simple, linear, static analysis to a complex, nonlinear, transient dynamic analysis. To provide needed information for validation, the experimental data was collected from the experiment conducted by Huang in 2002[10].

Description of CFST model:

- Concrete core : SOLID 65
- Steel tube : SHELL 181
- Medium mesh size
- Boundary condition – pinned at bottom
- Bonded interface contact between steel and concrete with coefficient of friction 0.25
- Axial load on rigid plate with pilot node with no separation contact
- Quarter of the square and circular CFST modelled with symmetric boundary condition

### 4.1 Modelling in ANSYS

Steel tube and concrete core are modelled using SHELL 181 and SOLID 65 respectively. Medium sized mesh is used. Bottom of CFST is hinged by restraining  $U_x$ ,  $U_y$  and  $U_z$ . Owing to symmetry of the specimen and boundary conditions, only quarter of the structure with symmetric

boundary conditions on the symmetric planes is modelled and analyzed.

The interface contact between steel tube and concrete core is modelled by TARGE170 and CONTA174, where a surface to surface contact is given. It is preferred to use more stiffer material as the target and the other one as contact surface[28]. Even though steel is stiffer than concrete, since the thickness of steel tube is very less compared to concrete, concrete is taken as the stiffer material.

Interface contact between CFST and rigid loading plate is modelled by TARGE170 and CONTA175, where a node to surface contact is given. Here rigid loading plate is taken as target and top surface of CFST as contact. Rigid plate with pilot node is given, so that load is applied on the pilot node to get an even distribution of the load on the structure.

TABLE-1. Details of experimental data

S.no	B or D (mm)	t (mm)	B/t or D/t	L (mm)	L/B	f <sub>y</sub> (MPa)	f <sub>c</sub> ' (MPa)
S 200	200	5	40	600	3	265.8	27.15
C 200	200	5	40	600	3	265.8	27.15

A circular and a square CFST with same depth, length, tube thickness, D/t and L/D ratios were selected for the validation. The simulation results show good agreement with the validation models.

TABLE-2. Comparison of analytical and experimental data

S.no	P <sub>(EXP)</sub> (kN)	P <sub>(ANL)</sub> (kN)	P <sub>Error</sub> %
S 200	2312	2294	1
C 200	2013	2001	1

## 4.2 Result and discussions

The distribution of the contact pressure between circular steel tube and core concrete is much more uniform than that between square steel tube and concrete, resulting in much higher confinement and more efficient interaction between steel tube and core concrete in circular CFST columns, as well as ultimate load capacity and ultimate displacement. The local buckling is more likely to occur in CFST columns with square cross-sections, as shown in chart.1, which gives the analysis results for S 200 and C 200. However, for the reasons of being easier in beam-to-column connection design and high cross sectional bending stiffness the square CFST is still increasingly used in construction.

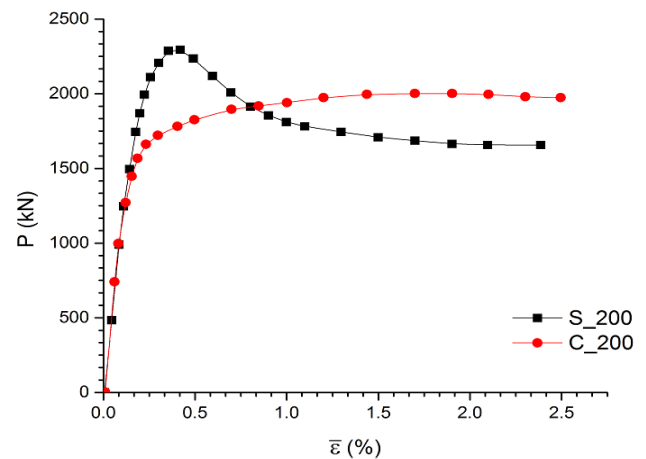


Chart-1. Load - Strain % graph of square and circular CFST of same D/t ratio

Comparing circular and square CFST of same D/t and L/D ratio, square CFST shows higher ultimate strength, due to increased area of cross-section. But after the ultimate strength square CFST shows sudden degradation of strength, (as shown in chart.1) this is due to the strain softening property of square section. But circular CFST closely approaches an elastic-perfectly plastic behaviour, ie. it shows strain hardening nature and have gradual degradation of strength. This is because (as shown in fig.3) the circular CFST columns have uniform confining pressure in all the radial direction, thus concrete core and steel tube contact entirely to each other and no local buckling of tubes take place, while in the square CFST column the steel tube confining pressure is high at the corners.

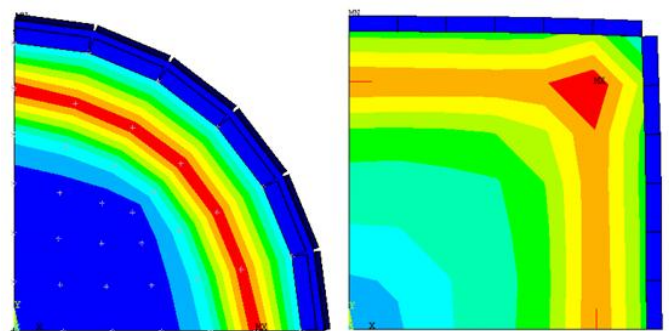


Fig.3. Stress distribution pattern in circular and square CFST

## 5. CONCLUSION

A nonlinear FEM based model has been developed using ANSYS for the numerical simulation of CFST specimens. The attempt to study the behaviour of square and circular CFST by cross-section shows reasonable results. The difference in behaviour of load-strain % curve is due to the reason that circular CFST columns have uniform confining pressure in all the radial direction, while in the square CFST column confining pressure is high at the corners.

## REFERENCES

- [1]. ACI-318-11. Building code requirements for structural concrete and commentary ACI Committee 318, Detroit (MI); 2011.
- [2]. DBJ/T13-51-2010. Technical Specifications for Concrete-Filled Steel Tubular Structures (Revised Version. Fuzhou, China: The Housing and Urban-Rural Development Department of Fujian Province; 2010.
- [3]. Eurocode 4. Design of composite steel and concrete structures, Part 1.1, general rules and rules for buildings, DD ENV 1994-1-1, London, United Kingdom; 1994.
- [4]. IS 13920 (1993): Ductile detailing of reinforced concrete structures subjected to seismic forces - Code of practice [CED 39: Earthquake Engineering]
- [5]. Richart, F. E., Brandtzaeg, A., and Brown, R. L., 1928, "A study of the failure of concrete under combined compressive stresses." *Bulletin 185*, University of Illinois Engineering Experimental Station, Champaign, Ill.
- [6]. Saenz, L. P., 1964, "Equation for the stress-strain curve of concrete." *ACI J.*, 61(9), pp 1229-1235.
- [7]. Elwi, A. A., and Murray, D. W., 1979. "A 3D hypoelastic concrete constitutive relationship." *J. Engrg. Mech. Div., ASCE*, 105(4), pp 623-641
- [8]. Stephen P. Schneider, 1988, "Axially Loaded Concrete-Filled Steel Tubes", *ASCE, J. Struct. Eng.*, 1998, 124(10): pp 1125-1138.
- [9]. Mirmirian, A., Zagers, K., Yuan, W., 2000. "Nonlinear finite element modelling of concrete confined by fiber composites". *Finite Element in Analysis and Design 35(1)*, pp 79-96. C angle
- [10]. C. S. Huang, Y.-K. Yeh, G.-Y. Liu, H.-T. Hu, K. C. Tsai, Y. T. Weng, S. H. Wang, M.-H. Wu, 2002, "Axial Load Behavior of Stiffened Concrete-Filled Steel Columns", *ASCE, Journal of Structural Engineering*, Vol. 128, No. 9, pp 1222-1230.
- [11]. Hsuan-Teh Hu, Chiung-Shiann Huang, Ming-Hsien Wu, Yih-Min Wu, 2003, "Nonlinear Analysis of Axially Loaded Concrete-Filled Tube Columns with Confinement Effect", *ASCE, J. Struct. Eng.*, 129, pp 1322-1329. F1 k3
- [12]. Kenji Sakino, Hiroyuki Nakahara, Shosuke Morino, and Isao Nishiyama, 2004, "Behavior of Centrally Loaded Concrete-Filled Steel-Tube Short Columns", *ASCE, J. Struct. Eng.*, 2004, 130 (2) pp 180-188
- [13]. J. Zeghiche, K. Chaoui, 2005, "An experimental behaviour of concrete-filled steel tubular columns", *Journal of Constructional Steel Research* 61, pp 53 - 66.
- [14]. Zhong Tao, Lin-Hai Han, Dong-Ye Wang, 2007, "Experimental behaviour of concrete-filled stiffened thin-walled steel tubular columns", *ELSEVIER, Thin-Walled Structure 45*, pp 517-527
- [15]. Z.H. Lu and Y.G. Zhao, 2008 "Mechanical Behavior And Ultimate Strength Of Circular CFT Columns Subjected To Axial Compression Loads", *The 14th World Conference on Earthquake Engineering*.
- [16]. Ying Wan , Yuan Xuan, Pengfei Mao, 2010, "Nonlinear Finite Element Analysis of the Steel-concrete Composite Beam to Concrete-filled Steel Tubular Column Joints," *International Journal of Nonlinear Science*, Vol.9(2010) No.3, pp.341-348
- [17]. Anil Kumar Patidar, 2012, "Behaviour of Concrete Filled Rectangular Steel Tube Column", *IOSR Journal of Mechanical and Civil Engineering*, Vol. 4, pp 46-52.
- [18]. Mohamed Mahmoud El-Heweity, 2012, "On the performance of circular concrete-filled high strength steel columns under axial loading", *Alexandria Engineering Journal* 51, pp 109-119.
- [19]. Haider M. Abdul Hussein, Ahmed N. Mohammed, 2013, "Nonlinear Finite Element Analysis of Concrete Filled Steel Tubes," *Journal of Babylon University/ Engineering Sciences / No.(2)/ Vol.(21): 2013*, pp 477- 492.
- [20]. Madiha Z.J. Ammari, Moayyad M. Al-Nasra, Abdelqader Najmi, 2013, *International Journal of Engineering Science Invention*, Vol. 2, Issue 4, pp.59-66
- [21]. Rajeshkumar.B, Anil Kumar Patidar and Helen Santhi. M, 2013, "FE Analysis Of Concrete Filled Cold Formed Steel Sections Using Ansys," *IJACE*, Vol.3, pp. 11-18
- [22]. Yahia Raad Abbas Alani, V.C. Agarwal, 2013, "Nonlinear Finite Element Study on the Circular Concrete Filled Steel Tubular Columns," *International Journal of Innovative Technology and Exploring Engineering (IJITEE)* ISSN: 2278-3075, Volume-3, Issue-6, November 2013, pp 52-55
- [23]. Zhong Tao, Zhi-Bin Wang, Qing Yu, 2013, "Finite element modelling of concrete-filled steel stub columns under axial compression", *ELSEVIER, Journal of Constructional Steel Research 89*, pp 121-131
- [24]. Ziyad A. Khaudhair, P.K. Gupta, A.K. Ahuja, 2013, "Parametric Investigations on Behaviour of Square CFST Columns", *International Journal Of Scientific & Engineering Research*, Vol. 4, Issue 5, pp 107 - 110
- [25]. Bhushan H. Patil, P. M. Mohite, 2014, " Parametric Study of Square Concrete Filled Steel Tube Columns Subjected To Concentric Loading", *Int. Journal of Engineering Research and Applications*, Vol.4, Issue 8, pp 109-112.
- [26]. Darshika k. Shah, M.D.Vakil, M.N.Patel, 2014, " Parametric Study of Concrete Filled Steel Tube Column", *IJEDR*, Volume 2, Issue 2, pp 1678 - 1682.
- [27]. Vipulkumar Ishvarbhai Patel, Qing Quan Liang, Muhammad N.S. Hadi, 2014, "Nonlinear analysis of axially loaded circular concrete-filled stainless steel tubular short columns", *ELSEVIER, Journal of Constructional Steel Research 101*, pp 9-18
- [28]. ANSYS Mechanical APDL Element Reference, Release 14.0.

**Notations**

$A_c$	cross-sectional areas of concrete	$f_y$	yielding stress of steel
$A_s$	cross-sectional areas of steel tube	$f_{cu}$	unconfined concrete cube compressive strength
$A_t$	total cross-sectional areas of steel tube and concrete	$f'_c$	unconfined concrete cylinder compressive strength
$D, B$	outer dimensions of the steel tube	$\epsilon'_c$	unconfined strain in concrete = 0.003
$c$	cohesion	$f'_{cc}$	confined concrete compressive strength
$\varphi$	angle of internal friction	$\epsilon'_{cc}$	confined strain
$\psi$	dilatancy angle	$f_y$	yield strength of the steel
$\xi_c$	confinement factor	$f_1$	lateral confinement pressure
$E_{cc}$	initial Young's modulus of confined concrete	$k_1, k_2$	confinement coefficients = 4.1 and 20.5 respectively
$E_s$	elastic modulus of the steel	$k_3$	degradation factor
$E'_s$	tangent modulus of steel after yielding = $0.01E_s$	$\mu_{cc}$	Poisson's ratio of confined concrete = 0.2
$\sigma_s$	steel stress	$R_E$	modular ratio
$\epsilon_s$	steel strain	$R_\sigma$	stress ratio = 4
$\sigma_y$	yielding strain of steel	$R_\epsilon$	strain ratio = 4
		$t$	wall thickness of the steel tube